

THE EFFECT OF GASDYNAMICS ON THE STRUCTURE OF DARK MATTER HALOS

Marcelo Alvarez^{1,2}, Paul R. Shapiro¹, and Hugo Martel¹

University of Texas at Austin

RESUMEN

El resumen será traducido al español por los editores.

Adaptive SPH and N-body simulations were carried out to study the effect of gasdynamics on the structure of dark matter halos that result from the gravitational instability and fragmentation of cosmological pancakes. Such halos resemble those formed in a hierarchically clustering CDM universe and serve as a test-bed model for studying halo dynamics. With no gas, the density profile is close to the universal profile identified previously from N-body simulations of structure formation in CDM. When gas is included, the gas in the halo is approximately isothermal, and both the dark matter and the gas have singular central density profiles which are steeper than that of the dark matter with no gas. This worsens the disagreement between observations of constant density cores in cosmological halos and the singular ones found in simulations. We also find that the dark matter velocity distribution is less isotropic than found by N-body simulations of CDM, because of the strongly filamentary substructure.

ABSTRACT

Adaptive SPH and N-body simulations were carried out to study the effect of gasdynamics on the structure of dark matter halos that result from the gravitational instability and fragmentation of cosmological pancakes. Such halos resemble those formed in a hierarchically clustering CDM universe and serve as a test-bed model for studying halo dynamics. With no gas, the density profile is close to the universal profile identified previously from N-body simulations of structure formation in CDM. When gas is included, the gas in the halo is approximately isothermal, and both the dark matter and the gas have singular central density profiles which are steeper than that of the dark matter with no gas. This worsens the disagreement between observations of constant density cores in cosmological halos and the singular ones found in simulations. We also find that the dark matter velocity distribution is less isotropic than found by N-body simulations of CDM, because of the strongly filamentary substructure.

Key Words: **COSMOLOGY: THEORY — GALAXIES: HALOES — GALAXIES: FORMATION — DARK MATTER**

1. INTRODUCTION

N-body simulations of structure formation that have as initial conditions a spectrum of density fluctuations consistent with a cold dark matter (CDM) universe have revealed that dark matter halos possess a universal density profile that diverges as $r^{-\gamma}$ near the center, with $1 \leq \gamma \leq 2$ (e.g. Navarro, Frenk, & White 1997 “NFW”; Moore *et al.* 1998). Much effort has been made attempting to understand the apparent discrepancy between

¹Department of Astronomy.

²Center for Computational Visualization, Texas Institute for Computational and Applied Mathematics.

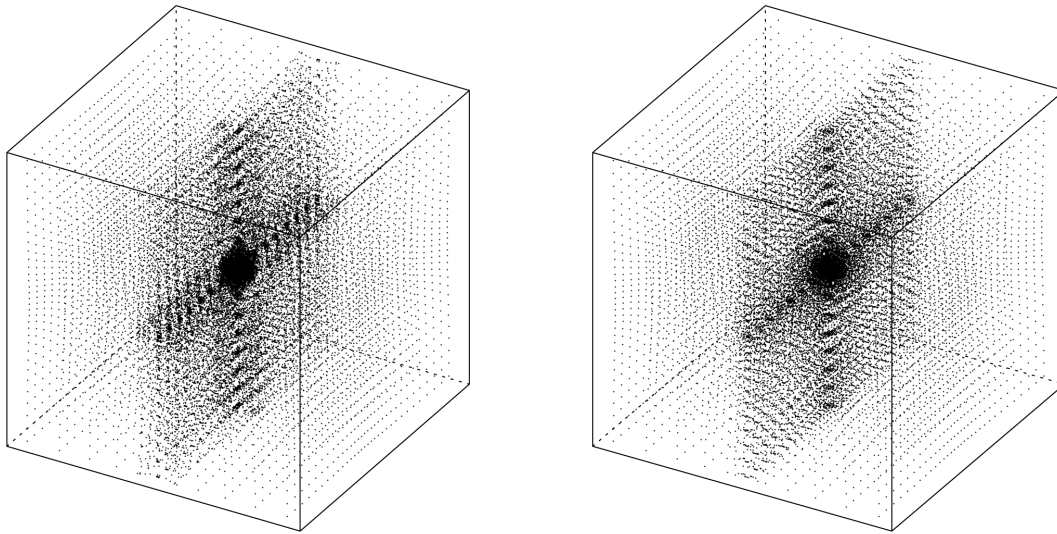


Fig. 1. Dark matter (left) and Gas (right) particle positions at $a/a_c = 3$ (volume = λ_p^3).

these singular density profiles found in N-body simulations and current observations of the rotation curves of nearby dwarf galaxies and of strong lensing of background galaxies by the galaxy cluster CL0024+1654 (Tyson, Kochanski, & dell’Antonio 1998), which suggest that cosmological halos of all scales have flat density cores, instead. Several ways to reconcile the theory with observations have been hypothesized, among which are:

- Problems with the N-body gravity solvers. Upon further scrutiny, however, the simulations have been found to represent faithfully the actual gravitational processes at work in hierarchical clustering.
- Self-interacting dark matter. If the dark matter is not collisionless as previously assumed but rather can interact nongravitationally with itself, this may change the dynamics in such a way as to produce constant density cores (Spergel & Steinhardt 2000).
- Gasdynamical effects due to the baryonic component. The inclusion of gas dynamics in the N-body simulations may lead to constant density cores.

It is the latter case which we address here. In particular, we analyze the density profiles of cosmological halos formed in numerical simulations of cosmological pancakes with and without a substantial baryonic component.

2. HALO FORMATION BY GRAVITATIONAL INSTABILITY DURING PANCAKE COLLAPSE

Consider the growing mode of a single sinusoidal plane-wave density fluctuation of comoving wavelength λ_p and dimensionless wavevector $\mathbf{k}_p = \hat{\mathbf{x}}$ (length unit = λ_p) in an Einstein-de Sitter universe dominated by cold, collisionless dark matter. Let the initial amplitude δ_i at scale factor a_i be chosen so that a density caustic forms in the collisionless component at scale factor $a = a_c = a_i/\delta_i$.

Pancakes modelled in this way have been shown to be gravitationally unstable, leading to filamentation and fragmentation during the collapse (Valinia *et al.* 1997). Such instability can be triggered if we perturb the 1D fluctuation described above by adding to the initial conditions two transverse, plane-wave density fluctuations with equal wavelength $\lambda_s = \lambda_p$, wavevectors \mathbf{k}_s pointing along the orthogonal vectors $\hat{\mathbf{y}}$ and $\hat{\mathbf{z}}$, and amplitudes $\epsilon_y \delta_i$ and $\epsilon_z \delta_i$, respectively, where $\epsilon_y \ll 1$ and $\epsilon_z \ll 1$. A pancake perturbed by two such density perturbations will be referred to as $S_{1,\epsilon_y,\epsilon_z}$. All results presented here refer to the case $S_{1,0.2,0.2}$ unless otherwise noted. Such a perturbation leads to the formation of a quasi-spherical mass concentration in the pancake plane at the intersection of two filaments (Figure 1). Halos formed from pancake collapse as modelled above have a

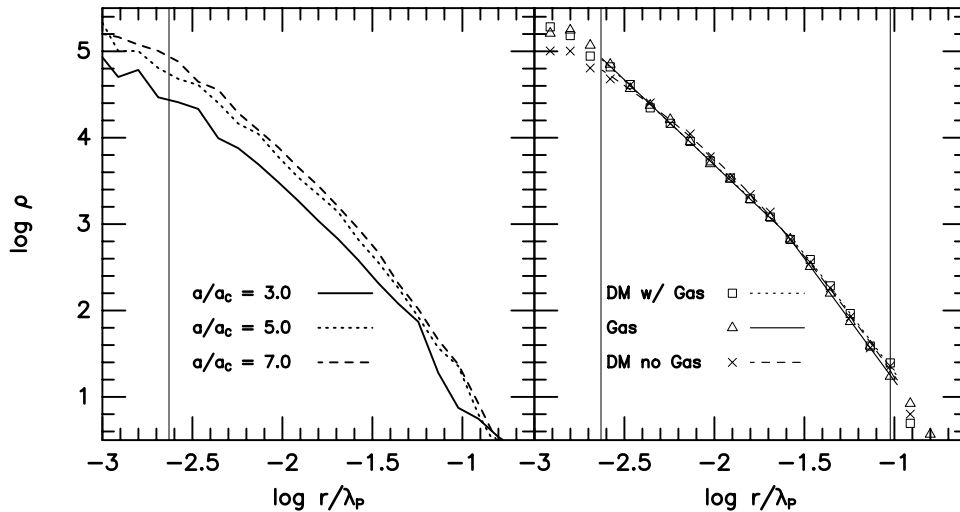


Fig. 2. (left) Evolution of dark matter density profile found by spherically averaging over logarithmically-spaced radial bins. (right) Density profiles for each component (in units of cosmic mean density for that component) at $a/a_c = 5.0$. Label “DM w/ Gas” means the dark matter profile in the simulation which includes gas.

density profile similar in shape to those found in simulations of hierarchical structure formation with realistic initial fluctuation spectra (Valinia 1996; Martel *et al.* 2000). As such, pancake collapse and fragmentation can be used as a test-bed model for halo formation which retains the realistic features of anisotropic collapse, continuous infall, and cosmological boundary conditions. Questions we seek to answer quantitatively are:

- Is the halo that results from pancake instability and fragmentation in a relaxed equilibrium state?
- How isotropic is the resulting velocity distribution for the dark matter, and how isothermal are the gas and dark matter?
- What effect does including gas in the simulations have on the dark matter density profile?

The pancake problem (without radiative cooling) is self-similar and scale-free, once distance is expressed in units of the pancake wavelength λ_p and time is expressed in terms of the cosmic scale factor a in units of the scale factor a_c at which caustics form in the dark matter and shocks in the gas. In the currently-favored flat, cosmological-constant-dominated universe, however, this self-similarity is broken because Ω_M/Ω_Λ decreases with time, where Ω_M and Ω_Λ are the matter and vacuum energy density parameters, respectively. For objects which collapse at high redshift in such a universe (e.g. dwarf galaxies), the Einstein-de Sitter results are still applicable as long as we take $(\Omega_B/\Omega_{DM})_{E-deS} = (\Omega_B/\Omega_{DM})_\Lambda$, where Ω_B and Ω_{DM} are the baryon and dark matter density parameters. If $\Omega_B = 0.045$, $\Omega_{DM} = 0.255$, and $\Omega_\Lambda = 0.7$ at present, then the E-deS results are applicable if we take $\Omega_B = 0.15$ and $\Omega_{DM} = 0.85$, instead.

3. RESULTS

The numerical technique used here to simulate the collapse and fragmentation of a cosmological pancake couples the gasdynamical method Adaptive Smoothed Particle Hydrodynamics (ASPH) (Shapiro *et al.* 1996; Owen *et al.* 1998) with a particle-particle, particle-mesh (P³M) N-body gravity solver (Martel & Shapiro 2000). Results presented here are for a simulation with 64^3 particles each of dark matter and gas when hydrodynamics is included, and 64^3 dark matter particles for the case with gravity only, on a P³M grid with 128^3 cells. We consider an Einstein-de Sitter universe ($\Omega_M = 1$, $\Omega_\Lambda = 0$) and two cases: $(\Omega_B, \Omega_{DM}) = (0, 1)$ or $(0.15, 0.85)$. The pancake-filament-halo structure of our results is illustrated by Figure 1. By $a/a_c = 5$, this halo contains approximately 10^5 particles each of dark matter and gas.

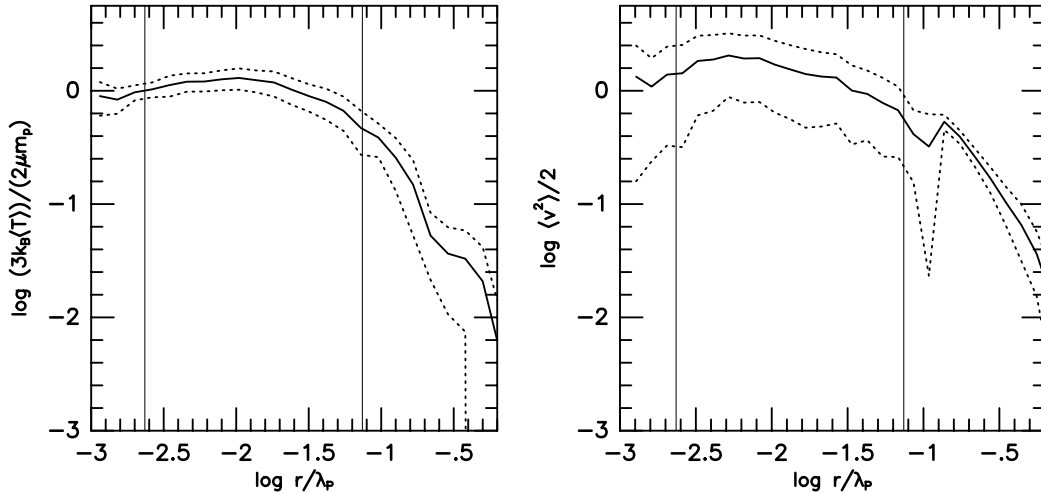


Fig. 3. At $a/a_c = 5.0$, Gas (left) and Dark Matter (right) specific thermal and kinetic energy profiles, respectively, in dimensionless computational units, at $a/a_c = 5.0$, which resulted from spherically averaging logarithmically-spaced radial bins. The dotted lines show the rms fluctuations. The two vertical lines in each denote the numerical softening length for the gravity calculation and r_{200} .

3.1. The equilibrium halo structure and similarity to CDM N -body simulation halos

The left panel of Figure 2 shows the evolution of the density profile of the dark matter halo in the simulation with no gas. By $a/a_c = 5$, the halo has asymptoted to an equilibrium profile. A χ^2 -minimization fit was performed on this profile over the range between the gravitational softening length r_{soft} and r_{200} , the radius within which the mean density is 200 times the cosmic mean density at that epoch, where $r_{soft}/\lambda_p \cong 2.3 \times 10^{-3}$ and $r_{200}/\lambda_p \cong 7.5 \times 10^{-2}$, for each component X of the matter density. The fitting function we use, in general, is of the form

$$\rho_X = \frac{\rho_s}{\left(\frac{r}{r_s}\right)^\gamma \left(1 + \left(\frac{r}{r_s}\right)^{1/\alpha}\right)^{\alpha(\beta-\gamma)}} \quad (1)$$

(Zhao 1996; Hernquist 1990), which approaches $\rho_X \propto r^{-\gamma}$ at $r \ll r_s$ and $\rho_X \propto r^{-\beta}$ at $r \gg r_s$, where ρ_X and ρ_s are in units of the mean cosmic density of component X at the same epoch. We found $\{\alpha, \beta, \gamma, r_s/\lambda_p, \rho_s\} = \{0.866, 3.18, 1.18, 1.39 \times 10^{-2}, 9.19 \times 10^3\}$. This profile is similar in shape to the universal density profile found for CDM halos by NFW based upon N -body simulations, for which $\{\alpha, \beta, \gamma\} = \{1, 3, 1\}$. In the notation of NFW, our best-fit halo concentration parameter, $c \equiv r_{200}/r_s$, is $c \cong 5$, while our ρ_s corresponds to NFW's δ_c . According to NFW, $\delta_c = (200/3)c^3/[ln(1+c) - c/(1+c)]$. For our value of $c \cong 5$, this yields $\delta_c \cong 9 \times 10^3$, very close to our best-fit value of ρ_s . Such a density profile is thus a more general outcome of cosmological halo formation by gravitational condensation, not limited to hierarchical clustering.

A common assumption is that “virialized” objects resulting from cosmological perturbations have an approximately isothermal temperature distribution and a dark matter velocity distribution that is isotropic. Figure 3 shows the spherically-averaged specific thermal energy of the gas ($\frac{3}{2}k_B\langle T\rangle/\mu m_p$) and kinetic energy of the dark matter ($\frac{1}{2}\langle v^2\rangle$). The gas in the halo is nearly isothermal from the softening length to r_{200} , with $\langle T(r_{soft})\rangle/\langle T(r_{200})\rangle \leq 2$. The dark matter kinetic energy follows a similar profile with a slightly steeper drop closer to the center. Figure 4 shows the parameter $\beta_{an} \equiv 1 - \langle v_t^2\rangle/2\langle v_r^2\rangle$, which is a measure of the anisotropy of the velocity distribution of the collisionless dark matter, as a function of distance from the center. In the limits of isotropic and radial motion, $\beta_{an} = 0$ and 1, respectively. The distribution is somewhat more anisotropic than usually found in hierarchical clustering simulations, due to the highly anisotropic infall which channels matter along the filaments that intersect at our halo, favoring radial motion. While this is true for both cases, the case with gas included seems to suppress radial motion at small radii.

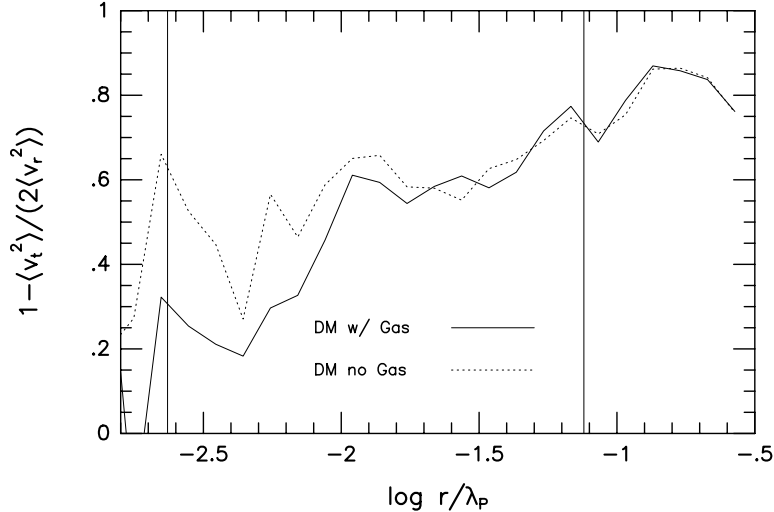


Fig. 4. The anisotropy parameter β_{an} for the dark matter in the cases with and without gas, calculated by spherically averaging the tangential and radial components within logarithmically-spaced radial bins.

3.2. Comparison of density profiles with and without gas

Figure 2 shows the profile fits for each component. The parameters $\{\alpha, \beta, \gamma, r_s/\lambda_p, \rho_s\}$ for each component are:

- Dark matter for N-body only: $\{0.866, 3.18, 1.18, 1.39 \times 10^{-2}, 9.19 \times 10^3\}$
- Dark matter for N-body/Gas: $\{0.141, 2.78, 1.95, 2.82 \times 10^{-2}, 6.15 \times 10^2\}$
- Gas: $\{3.07 \times 10^{-3}, 2.84, 1.98, 2.47 \times 10^{-2}, 8.06 \times 10^2\}$

The density profiles shown in the right panel of Figure 2 show that when gas is added to the simulation, the dark matter density profile steepens at the center. The dark matter parameter γ , the negative of the asymptotic logarithmic slope for inner radii, is 1.18 for the case with no gas and 1.95 for the case with. While the fitting function does not make a direct comparison of the fits at inner radii easy because of the difference in scale radius r_s for each component, it does show that the halo in the case with gas has a steeper inner slope. As such, this effect can only worsen the disagreement between the predicted singular profiles and observations of constant density cores. More detailed analysis at higher resolution is needed before this conclusion can be made with certainty, since the part of the profile in question is at radii very close to the numerical softening length for the gravity calculation, even though there were more than 10^5 particles each of gas and dark matter within r_{200} at this epoch.

4. SUMMARY AND DISCUSSION

We have analyzed the structure of the halo which forms by gravitational instability when a cosmological pancake is perturbed during its collapse, based upon ASPH/P³M simulations. Such halos resemble those formed in CDM simulations, with a density profile like that of NFW, when no gas is included. Our results strengthen the conclusion reached elsewhere that halos with a universal structure like that identified by NFW arise from gravitational instability under a wider range of circumstances than those involving hierarchical clustering (e.g. Huss, Jain, & Steinmetz 1999; Moore *et al.* 1999; Tittley & Couchman 1999). When gas is included, we find that the halo gas acquires a steeper inner profile than that of the pure N-body results, almost as steep as $\rho \propto r^{-2}$, as does the dark matter in this case. The halo appears to be in a quasi-isothermal equilibrium state, although matter continues to fall into the halo, mainly along the filaments. The persistence of filamentary

substructure in the halo seems to manifest itself by sustaining the radial motion of the infalling particles even after “virialization”, in contrast to results found from simulations of hierarchical clustering (Eke, Navarro, & Frenk 1998). The inclusion of gas lessens this effect somewhat at the center of the halo.

Our result that the presence of a gasdynamical component steepens the inner profile of the dark matter halo relative to the pure N-body result is consistent with some other recent simulations of cluster formation in the CDM model (e.g Lewis *et al.* 1999). Tittley and Couchman (1999) report $\rho_{DM} \propto r^{-1.8}$ at small r in their simulations, in rough agreement with our result, although they note that the NFW profile is also a reasonable fit. However, for CDM-like initial conditions, they actually report a steeper inner profile for the gas than for the dark matter, while our gas and dark matter inner profiles are equally steep. CDM simulations of a single cluster by many different codes, summarized in Frenk *et al.* (2000), report somewhat different results from those of Tittley and Couchman (1999). In particular, while the dark matter profile was found in Frenk *et al.* (2000) to be well-fit by the NFW profile when gas was included, the gas density profile was even flatter than this at small radii. Lewis *et al.* (1999) also find a gas density inner profile which is flatter than that of the dark matter. It would be tempting to attribute the difference between our result that the density profiles of both gas and dark matter are steeper than NFW when gas is included, and the flatter inner profiles reported in Frenk *et al.* (2000), to the difference between CDM-like and pancake-instability initial conditions. However, this would not explain the difference between the results of Frenk *et al.* (2000) and Tittley and Couchman (1999), both for CDM initial conditions.

This work was supported in part by grants NASA NAGC-7363 and NAG5-7821, Texas ARP No. 3658-0624-1999, and NSF SBR-9873326 and ACR-9982297.

REFERENCES

- Eke V.R., Navarro J.F., and Frenk C.S. 1998, ApJ 503, 569
 Frenk C.S. *et al.* 2000, ApJ 525, 554
 Hernquist, L., 1990, ApJ, 356, 359
 Huss A., Jain B., and Steinmetz M. 1999, ApJ, 517, 64
 Lewis G.F., Babul A., Katz N., Quinn T., Hernquist L., and Weinberg D.H. 1999 astro-ph/9907097
 Martel H. and Shapiro P.R. 2000, in preparation
 Martel H., Shapiro P.R., and Valinia A. 2000, in preparation
 Moore B., Governato F., Quinn T., Stadel, J. and Lake, G. 1998, ApJL, 499, 82
 Moore B., Quinn T., Governato F.J., Stadel J., and Lake G. 1999, MNRAS, 310, 1147
 Navarro J.F., Frenk C.S., and White S.D.M. 1996, ApJ, 462, 563
 Navarro J.F., Frenk C.S., and White S.D.M. 1997, ApJ, 490, 493
 Owen J.M, Villumsen J.V., Shapiro P.R., and Martel H. 1998, ApJS, 116, 155
 Shapiro P.R., Martel H., Villumsen J.V., and Owen, J.M. 1996, ApJS, 103, 269
 Spergel D.N. and Steinhardt P.J. 2000, Phys.Rev.Lett., 84, 3760
 Tittley E.R. and Couchman H.M.P. 1999, astro-ph/9911460
 Tyson J.A., Kochanski G.P., and dell’Antonio I.P. 1998, ApJ, 498, L107
 Valinia A. 1996, Ph.D. Dissertation, University of Texas at Austin
 Valinia A., Shapiro P.R., Martel H., and Vishniac E.T. 1997, ApJ, 479, 46
 Zhao H.S. 1996, MNRAS, 278, 488